Vibronic Relaxation of Polyatomic Molecule in Nonpolar Solvent: Femtosecond Anisotropy/Intensity Measurements of the S_n and S_1 Fluorescence of Tetracene

Nilmoni Sarkar,† Satoshi Takeuchi, and Tahei Tahara*

Institute for Molecular Science (IMS), Myodaiji, Okazaki 444-8585, Japan

Received: February 24, 1999; In Final Form: April 20, 1999

The electronic and vibrational relaxation of tetracene have been studied in solution by femtosecond time-resolved fluorescence spectroscopy. Tetracene was initially photoexcited to the highly excited singlet (S_n) state, ^1B_b, and the dynamics of the fluorescence from the ^1B_b state and the ^1L_a state (S_1) were investigated by fluorescence up-conversion. The fluorescence from the ^1B_b state was observed in the ultraviolet region, and its lifetime was determined as ∼120 fs. The anisotropy of the ^1B_b fluorescence was close to 0.4, which assured that the fluorescence is emitted from the excited state that was prepared by photoexcitation. The visible fluorescence from the ^1L_a state showed a finite rise that agreed well with the decay of the ^1B_b fluorescence. Negative anisotropy was observed for the ^1L_a fluorescence, reflecting that the ^1L_a transition moment is parallel to the short axis of the molecule and hence perpendicular to the ^1B_b transition moment. The anisotropy of the ^1L_a fluorescence, however, showed a very characteristic temporal behavior in the femtosecond time region: it exhibited a very rapid change and reached a certain value that is deviated from −0.2. The anisotropy data indicate that the ^1L_a fluorescence contains not only a short-axis polarized component but also a long-axis polarized component and that the ratio between the two components depends on both time and wavelength. The long-axis polarized component in the ^1L_a fluorescence was assigned to the ^1B_b-type fluorescence that appears as the result of the vibronic coupling between the ^1L_a state and the ^1B_b state. The observed initial rapid change of the anisotropy suggests that the highly excited vibrational states in the ^1L_a state which are strongly coupled with the ^1B_b state are first populated preferentially when the molecule is relaxed from the ^1B_b state to the ^1L_a state. The visible fluorescence anisotropy vanishes gradually because of the rotational diffusion in a few tens of picoseconds. In the picosecond region, we also observed additional dynamics in the fluorescence intensity whose time constant was about 12 ps. This dynamics was assigned to the vibrational relaxation (cooling) in the ^1L_a state. A series of relaxation processes taking place after photoexcitation of the molecule in solution are discussed.

1. Introduction

In most all steady-state fluorescence spectra of polyatomic molecules in solutions, only fluorescence from the lowest excited singlet (S_1) state is observed even when the molecule is initially photoexcited to the highly excited singlet (S_n, $n \geq 2$) state. This fact is widely accepted as a common rule in fluorescence spectroscopy under the name of Kasha's rule.[1] The rigidity of this rule is known to be very high although there are a few exceptional molecules such as azulene exhibiting the S_2 fluorescence.[2,3] The physical implication of Kasha's rule is that the electronic relaxation from the S_n state to the S_1 state takes place in a short time in comparison with the lifetime of the S_1 state. In other words, the S_n state can emit fluorescence only in very short period before the electronic relaxation so that the time-integrated intensity of the S_n fluorescence is negligibly small compared with that of the S_1 fluorescence. Therefore, the S_n fluorescence becomes noticeable only in some measurements undertaken with special care.[4,5]

In time-resolved measurements, however, when the time resolution exceeds the time constant of the $S_n \rightarrow S_1$ internal conversion, we can expect to observe the fluorescence from the highly excited state before the electronic relaxation. This situation is realized in femtosecond time-resolved measurements because typical lifetimes of the highly excited states are estimated to be in the range between ∼ 0.01 and 1 ps.[1,6] In fact, for example, we recently observed the fluorescence from the highly excited singlet states that appear in the course of photochemical reactions when we studied all-trans retinal[7,8] and 7-azaindole dimer.[9,10] It can be said that the observation of fluorescence from the highly excited singlet state is a common subject in femtosecond time-resolved fluorescence measurements although the number of relevant reports is still very limited.[11−16] In this sense, fluorescence spectroscopy can be a powerful tool in the femtosecond time region not only for studying the S_1 state dynamics but also for examining the highly excited singlet states and their relaxation dynamics. The relaxation process of the highly excited electronic states and the fate of the excess energy (dissipation) are very fundamental problems for the physicochemical study of photochemistry. It is clear that the detailed information about these processes is indispensable for full understanding of photochemistry in solution.

In this paper, we report our femtosecond time-resolved fluorescence study of the relaxation process of tetracene which successively takes place after photoexcitation. We excite the molecule to the S_n state by direct photoexcitation and examine the dynamics of both the S_n fluorescence and the S_1 fluores-

* To whom correspondence should be addressed.
† Present address: Indian Institute of Technology, Kharagpur, India.

10.1021/jp9906785 CCC: $18.00
Published on Web 06/06/1999

cence. We chose tetracene as a sample for the following several reasons. First, the electronic origins of the low-lying optical transitions in this molecule are well-known. Tetracene is a linear condensed aromatic system (polyacene), and the electronic spectroscopy as well as its photophysics have been studied in gas, solution, crystal, and also in thin film.[17−27] Especially, absorption spectra in solution and the electronic origin of the absorption bands have been discussed systematically by Platt on the basis of the perimeter model.[17,18] Second, the S_1 and the S_n transitions of tetracene in solution are well separated in energy, and the absorption maximum of a $S_n \leftarrow S_0$ transition matches the third harmonic of a Ti:sapphire laser that we use in our experimental setup as a light source. Third, tetracene has high symmetry, which allows us to get clear information from the anisotropy measurements. The fluorescence anisotropy measurements of polyatomic molecules in solution have been carried out extensively in the picosecond time region so far, mainly in order to obtain information about the rotational diffusion.[28] In the femtosecond time region, however, the rotation of the molecule is not important so that the anisotropy measurement affords more direct information about the transition moment direction of the electronic excited state that is responsible for the fluorescence emission.[10,29] Thus, we can take advantage of the anisotropy measurements to get information about the electronic relaxation dynamics, especially for a highly symmetric molecule like tetracene.

2. Experimental Section

The experimental setup for fluorescence up-conversion measurements has been already described in detail elsewhere.[7] Briefly, a mode-locked Ti:sapphire laser (Coherent, MIRA-900F) pumped by an argon ion laser (Coherent, INNOVA-310) is used as a light source. The output wavelength is tuned to 820 nm in the present measurements. The oscillator laser produces a 700 mW pulse train with a typical pulse duration of 55 fs. The third harmonic pulse (λ = 273 nm, 20 mW) is generated by using a LBO (1 mm thickness) and a BBO (1 mm thickness) crystal. It is focused into a thin-film jet stream of the sample solution for photoexcitation. The residual fundamental pulse is used as a gate pulse for the up-conversion process. The fluorescence emission is collected and focused into a BBO mixing crystal (0.5 mm thickness) with use of an aluminum coated elliptic mirror. A cutoff filter or a band-pass filter is placed between the mirror and the mixing crystal. The fluorescence is up-converted via type-I sum frequency generation with the gate pulse in the mixing crystal. The up-converted signal is separated from the other light by using an iris, a band-pass filter, and a 0.32-m monochromator (Jobin Yvon, HR-320) and finally is detected by a photon-counting photomultiplier (Hamamatsu, R585) with a counter (Stanford Research Systems, SR 400). Time-resolution was estimated from the difference-frequency generation (cross-correlation) between the pump pulse and the gate pulse. The observed cross-correlation function was well represented by a Gaussian function with full width at half-maximum of 280 fs.

The fluorescence detection at the magic angle, parallel and perpendicular conditions, was achieved by rotating the excitation polarization with respect to the gate polarization. The up-converted fluorescence intensities were measured with parallel and perpendicular conditions at each delay time. Since the up-conversion process acts as a "polarizer" in the fluorescence detection, we did not use any polarizer to select the fluorescence polarization. In fact, for the visible fluorescence, although we also carried out measurements in which a commercial film polarizer was placed before the mixing crystal, the obtained anisotropy value was essentially the same.

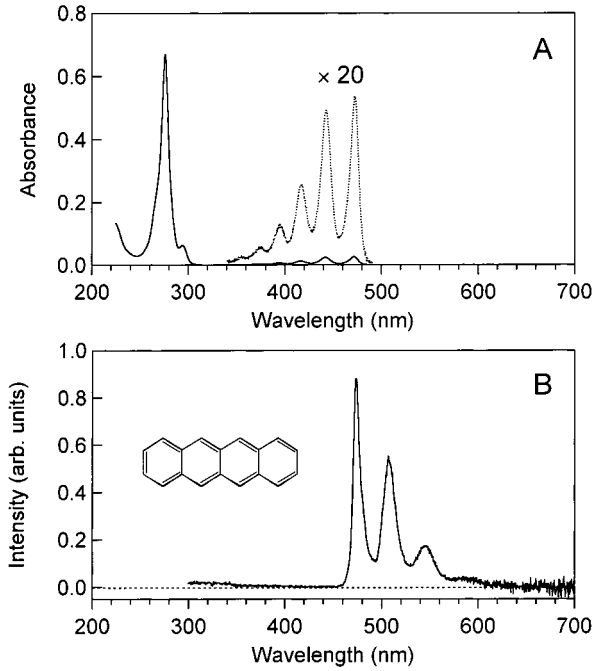

Figure 1. Stationary spectra of tetracene in hexadecane. (A) Ultraviolet−visible absorption spectrum. The dotted curve shows a visible portion of the spectrum magnified by 20 times. (B) Fluorescence spectrum obtained from 2.9×10^{-7} mol dm^{-3} solution (273 nm excitation). The molecular structure of tetracene is also depicted in the inset.

Steady-state absorption and fluorescence spectra were recorded with commercial spectrometers (Hitachi U-3500 and Spex Fluorolog-2). The fluorescence spectrum was corrected for spectral sensitivity of the instrument and was obtained as a photon-number-intensity spectrum.

Tetracene (2,3-benzanthracene, naphthacene) was purchased from Aldrich Chemical Co. and was sublimed in a vacuum before use. Hexadecane (anhydrous, 99+%) and heptane (special grade) were purchased from Aldrich and Wako Chemicals, respectively, and they were used without further purification. Since the solubility of tetracene in hexadecane is much higher than that in heptane, hexadecane was mostly used as solvent in the present study. A typical concentration of hexadecane solution was 2.9×10^{-5} mol dm^{-3}. A fresh sample solution was prepared for each time-resolved measurement.

3. Results and Discussion

3-1. Steady-State Spectra. Figure 1A depicts the absorption spectrum of tetracene in hexadecane. In this spectrum, the strongest sharp band is peaked around 273 nm. This absorption band has been assigned to the $^1B_b \leftarrow S_0$ transition. A weak absorption showing clear vibrational structure around 450 nm is due to the $^1L_a \leftarrow S_0$ transition. It is known that the transition moment relevant to the $^1B_b \leftarrow S_0$ absorption is parallel to the long axis of the molecule whereas that of the $^1L_a \leftarrow S_0$ absorption is perpendicular (parallel to the short axis). Another transition, the $^1L_b \leftarrow S_0$ transition, exists in this energy region of the polyacene system. In tetracene, however, this transition is believed to be located in a slightly higher energy region than the $^1L_a \leftarrow S_0$ transition and masked by the $^1L_a \leftarrow S_0$ absorption because of its very small oscillator strength.[17,18] In the present study, we excite tetracene through the strongest $^1B_b \leftarrow S_0$ transition located in the ultraviolet. Figure 1B shows the steady-state (time-integrated) fluorescence spectrum obtained with the

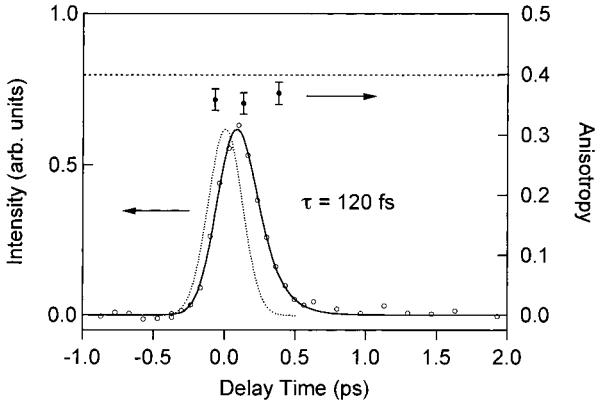

Figure 2. Up-converted signal obtained from tetracene in hexadecane (2.9×10^{-5} mol dm^{-3}) for fluorescence wavelength of 340 nm with 273 nm excitation (open circle). The dotted curve shows the instrumental response, and the solid curve represents the best-fitted exponential decay with a time constant of 120 fs. Fluorescence anisotropy values measured at three delay times are also shown (solid circle).

273-nm excitation. A fluorescence band appears around 500 nm and it exhibits clear vibrational structure. The spectral feature is close to the mirror image of the $^1L_a \leftarrow S_0$ absorption, indicating that the fluorescence is emitted predominantly from the ^1L_a state, the lowest excited singlet state of tetracene.

3-2. Ultraviolet Fluorescence Dynamics. Although the ^1L_a fluorescence is predominant in the steady-state fluorescence spectrum, the fluorescence emitted from the initially prepared ^1B_b state is expected to be observed in very early time after photoexcitation if the time-resolution of the measurement is sufficiently high. We searched for the ^1B_b fluorescence in the ultraviolet region with femtosecond time-resolution and found a very fast signal at the blue edge of our instrumental limit. Figure 2 shows the signal observed at 340 nm (magic angle configuration). The lifetime of this signal is so short that the time-resolved trace looks close to the instrumental response. However, it exhibits a slightly asymmetric feature, which indicates finite lifetime of this signal. Fitting analysis taking account of the instrumental response evaluated the lifetime of this ultraviolet signal as 120 fs.

Time-resolved measuremets were also carried out at parallel ($I_{\parallel}$) and perpendicular ($I_{\perp}$) conditions. The anisotropy values, which are defined as

$$r(t) = \frac{I_{\parallel}(t) - I_{\perp}(t)}{I_{\parallel}(t) + 2I_{\perp}(t)} \quad (1)$$

were determined at three different time delays and they are also plotted in Figure 2. As clearly seen, they are essentially the same. The obtained value of ~0.36 is very close to the theoretical value of 0.4 which is expected for the case that the fluorescence transition moment is parallel to the absorption transition moment. Thus, the anisotropy data strongly support that the observed ultraviolet signal is due to the fluorescence from the ^1B_b state that is initially prepared by the photoexcitation. Small deviation of the experimental value from the theoretical one is probably due to the finite solid angle of fluorescence collection which induces some contribution from the other polarization component. An excited state having a small oscillator strength has been suggested to be located slightly below the ^1B_b state.[19] However, the observed fluorescence is not from this state, because its transition moment is perpendicular to the long axis of the molecule and hence perpendicular to the transition moment of the ^1B_b absorption.

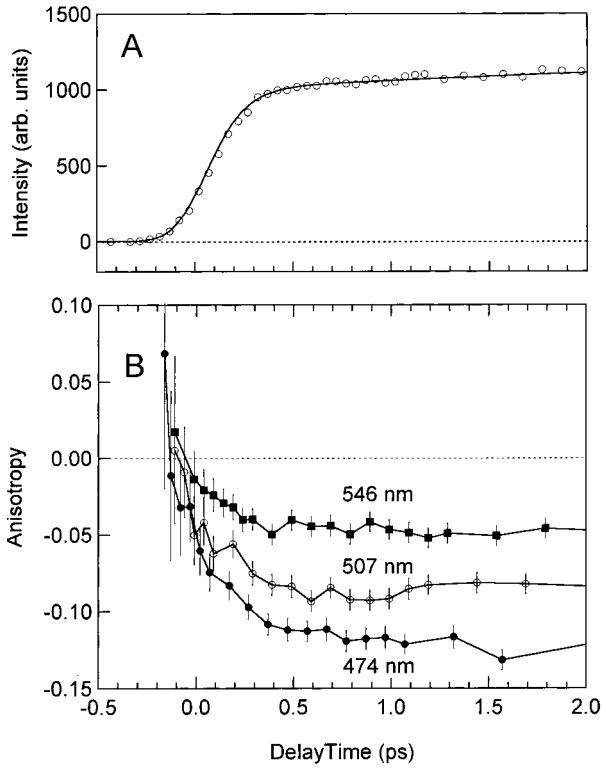

Figure 3. Early-time dynamics of the fluorescence intensity and anisotropy obtained from tetracene in hexadecane (2.9×10^{-5} mol dm^{-3}, 273 nm excitation). (A) Time-resolved fluorescence signal at 507 nm measured with the magic angle condition. The solid curve shows the best fitted curve that takes account of the 108 fs rise as well as the 12 ps dynamics (see text). (B) Time-resolved fluorescence anisotropy measured at three different wavelengths (474, 507, and 546 nm).

The oscillator strength of the strong ^1B_b transition is reported as 1.3.[19] This large oscillator strength means that the time-resolved intensity of the ^1B_b fluorescence can be high even though its lifetime is very short. However, the ^1B_b fluorescence observed at 340 nm was much weaker than we expected. It is highly likely that we observed a red tail of the ^1B_b fluorescence and that its intensity maximum is located in shorter wavelength region which we cannot measure with our present setup. The oscillator strength of 1.3 corresponds to the radiative lifetime of 0.86 ns if we use the frequency at the absorption peak as the frequency of the transition. The quantum yield of the ^1B_b fluorescence can be calculated as the ratio between the observed lifetime and the radiative lifetime, and it is estimated as low as 1.4×10^{-4}.

3-3. Femtosecond Visible Fluorescence Dynamics. Next we examined the dynamics of the ^1L_a fluorescence in the visible region. Figure 3A shows time-resolved fluorescence trace in early delay time measured at 507 nm (magic angle condition). The observed visible fluorescence shows a finite rise having a time constant of 108 fs. The rise of the visible fluorescence was analyzed also for other two wavelengths at 546 and 474 nm, and we obtained the rise time of 100 ± 20 fs as an average. The good agreement between the rise of the visible ^1L_a fluorescence and the decay of the ultraviolet ^1B_b fluorescence indicates that the ^1L_a state is populated in accordance with the decay of the ^1B_b state.

The fluorescence behavior due to the $^1B_b \rightarrow {}^1L_a$ electronic relaxation process looks simple if we see only the fluorescence data taken with the magic angle condition. However, the fluorescence anisotropy data revealed that profound dynamics

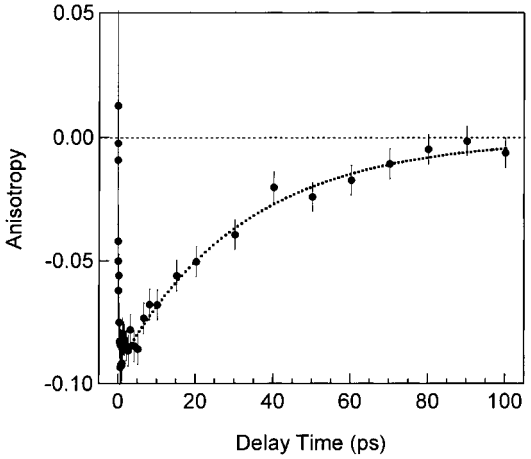

Figure 4. Temporal change of the fluorescence anisotropy at 507 nm in the picosecond time range. The dotted curve represents the best-fitted exponential function with a time constant of 32 ps.

exists in the course of the $^1B_b \rightarrow {}^1L_a$ relaxation. The fluorescence anisotropy data in the early time delay up to 2 ps are depicted in Figure 3B. It is clear that the anisotropy of the visible fluorescence is negative in this time range. The obtained negative anisotropy indicates that the orientation of the fluorescence transition moment is significantly deviated from the absorption transition moment. As described in section 3-1, the transition moment of the ^1L_a state is parallel to the short axis of the molecule, and hence perpendicular to the transition moment of the ^1B_b absorption. Therefore, the observation of the negative anisotropy is not surprising in itself. However, the following two points should be noted for the observed anisotropy data. First, the fluorescence anisotropy shows very rapid change before 1 ps and then reaches a plateau. Second, even the anisotropy value in the plateau region is significantly deviated from -0.2, which is the theoretical value expected for the "pure" short-axis polarized ^1L_a fluorescence. We confirmed the reproducibility of the anisotropy data by repeating experiments for several times. For the discrepancy between the experimental anisotropy value and the theoretical value, we first suspected that it was due to the finite solid angle of fluorescence collection, i.e., the contribution from the other polarization component. To check this possibility, we carried out anisotropy measurements for other fluorescence wavelengths using exactly the same optical configuration (except for the angle of the mixing crystal and the position of the monochromator). The fluorescence anisotropy data obtained at 474 and 546 nm are also shown in Figure 3B. The fluorescence anisotropy at the three wavelengths shows similar temporal change but its value significantly varies depending on the fluorescence wavelength. If the deviation from the theoretical value is merely due to the optical configuration of the experimental setup, the anisotropy values should be the same among these three wavelengths. Thus, it can be concluded that the visible fluorescence contains not only a "short-axis polarized component" which originates from the transition moment parallel to the short axis of the molecule. It also has a "long-axis polarized component" that is due to the transition moment parallel to the long axis. The data show that the relative magnitude between these two components depends on both delay time and fluorescence wavelength. We should note that the orientational motion of the molecule is not important in this early delay time region, as described in the next section.

3-4. Picosecond Visible Fluorescence Dynamics. The temporal change of fluorescence anisotropy at 507 nm is shown in Figure 4 for the time range up to 100 ps. The anisotropy

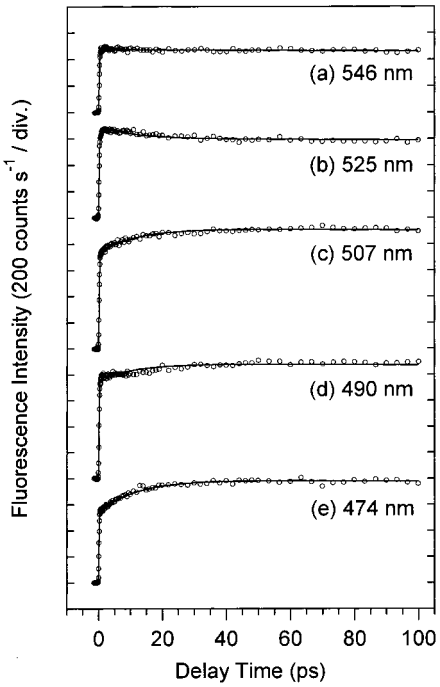

Figure 5. Up-converted fluorescence signals in the picosecond time range obtained from tetracene in hexadecane (2.9×10^{-5} mol dm^{-3}, 273 nm excitation). The signal traces are shown for fluorescence wavelengths of 546 (a), 525 (b), 507 (c), 490 (d), and 474 nm (e). The open circles are experimental data points, and the solid curves are results of the fitting analysis.

value reaches its negative maximum around 1 ps, and then it vanishes gradually. The slow disappearance of the fluorescence anisotropy was well fitted to a single-exponential function having a time constant of about 30 ps (the dotted curve). This time constant is ascribable to the orientational diffusion time of tetracene in hexadecane.[30,31] For comparison, the fluorescence anisotropy measurement was also carried out in heptane that is much less viscous than hexadecane. Owing to the poor solubility of tetracene in heptane (0.6×10^{-5} mol dm^{-3}), the signal-to-noise ratio of the time-resolved fluorescence data was significantly lower than that in hexadecane. Nevertheless, it was confirmed that the time constant for the disappearance of the negative anisotropy (orientational diffusion time) is significantly shortened to about 13 ps, reflecting the difference in the viscosity between heptane ($\eta = 0.34$) and hexadecane ($\eta = 3.34$).

The visible fluorescence intensity itself also exhibits characteristic temporal behavior in the picosecond time region. Figure 5 shows time-resolved fluorescence signals observed at five different wavelengths (magic angle configuration). It is clearly seen that the time-resolved fluorescence signal exhibits either a rise or a decay in the picosecond time range, depending on the wavelength. The signals at 474, 490, and 507 nm exhibit a rise followed by a long-lived component, whereas the signals at 525 and 546 nm show a decay followed by a long-lived component. The decay of the long-lived component is negligible in this time range because the lifetime of the ^1L_a fluorescence is as long as 5 ns in nonpolar solvent.[32,31] We fitted single-exponential functions to the rise/decay features by using a single time constant for all wavelengths and obtained a value of 12 ps as the characteristic time of this dynamics. Since (1) both rise and decay features are observed within the ^1L_a fluorescence band, and (2) tetracene is chemically inert in hexadecane, we concluded that this dynamics is not due to the population dynamics but arises from the spectral change of the ^1L_a fluorescence band.

In this experiment, tetracene is initially photoexcited to the ^1B_b state, so that the molecule gains the excess energy of more than 15000 cm^{-1} after the $^1B_b \rightarrow {}^1L_a$ relaxation. Therefore, the solute molecule in the S_1 (^1L_a) state is locally heated and then the excess energy is dissipated into the surrounding solvent. It is known that the vibrational cooling process gives rise to spectral change of the time-resolved fluorescence. For instance, Maroncelli and co-workers[33] observed the spectral change occurring in a ~10 ps time scale for Coumarin 153 fluorescence in cyclohexane and attributed it to the vibrational relaxation in the S_1 state. We also observed similar phenomena for the tautomer fluorescence of 7-azaindole dimer, which are ascribable to the vibrational cooling after proton-transfer reaction.[10] In addition, Iwata and Hamaguchi[34] recently reported their systematic work on the vibrational relaxation (cooling) of S_1 trans stilbene in solution with use of picosecond time-resolved Raman spectroscopy. They found a good correlation between the cooling rate of the solute molecule and the thermal diffusivity of the solvent and reported that the vibrational cooling takes place with a time constant of about 10 ps in nonpolar solvent (13 ps in heptane and 11 ps in hexane). Since the time constant of the fluorescence intensity change observed in the present study agrees well with a typical time constant of the vibrational cooling process in solution,[35] it is safely concluded that the observed 12-ps fluorescence dynamics is due to the vibrational cooling process in the S_1 (^1L_a) state of tetracene.

3-5. Electronic Relaxation and Vibronic Coupling. Now, we discuss anisotropy of the visible ^1L_a fluorescence in the femtosecond time region. As described in section 3-3, fluorescence anisotropy in the visible region shows a very rapid change after photoexcitation, and it reaches a particular negative value that is deviated from −0.2. Since tetracence is a highly symmetric molecule (D_{2h} symmetry), the transition moment relevant to the optical transition lying in the ultraviolet−visible region is orientated along either the long or the short axis of the molecule. Therefore, if the fluorescence emission is ascribable to the nature of a single electronic state, the anisotropy value should be either 0.4 (long-axis polarized transition), or −0.2 (short-axis polarized transition) in the early time region when rotational diffusion of the molecule can be neglected (note that we excite the molecule through the long-axis polarized $^1B_b \leftarrow S_0$ transition). The present anisotropy measurements clarified that the visible fluorescence contains not only a short-axis polarized component but also a long-axis polarized component, and that the relative magnitude between these two depends on both delay time and fluorescence wavelength. When the fluorescence consists of these two components, the anisotropy value can be related to the ratio (R) of the long-axis polarized component in the whole fluorescence intensity as follows:[36]

$$r = \frac{2I^{\text{long}} - I^{\text{short}}}{5I^{\text{long}} + 5I^{\text{short}}} = \frac{3R - 1}{5} \tag{2a}$$

where

$$R = \frac{I^{\text{long}}}{I^{\text{long}} + I^{\text{short}}} \left(= \frac{5r + 1}{3}\right) \tag{2b}$$

Here, I^{long} and I^{short} denote the intensities of the fluorescence from the molecule, which are due to the long-axis polarized transition moment and the short-axis polarized transition moment, respectively. In this formula, we neglect the effect of rotational diffusion of the molecule because we now focus on the anisotropy value in very early delay time. As the initial change finishes, the anisotropy values become about −0.05, −0.09, and −0.12 in the time region around 1 ps at the fluorescence wavelengths at 546, 507, and 474 nm, respectively. It means that the visible fluorescence contains ~ 25% (546 nm), ~ 18% (507 nm), and ~ 13% (475 nm) long-axis polarized component at each wavelength.

In tetracene, the ^1L_b state is believed to be located in a slightly higher energy region than the ^1L_a state. Therefore, we first suspected that the parallel component observed in the visible fluorescence might be the fluorescence from the ^1L_b state since the $^1L_b \leftarrow S_0$ transition is parallel to the long axis of the molecule (and hence parallel to the $^1B_b \leftarrow S_0$ transition). However, this possibility has been readily ruled out by the following two arguments. First, the oscillator strength of the ^1L_b state of polyacene is generally 2 orders of magnitude smaller than that of the ^1L_a state.[17,18] Thus, it is very unlikely that the ^1L_b fluorescence can give noticeable contribution to the observed anisotropy, even if it exists. Second, if the long-axis polarized component is due to the ^1L_b fluorescence, it should be larger at shorter wavelength since the ^1L_b fluorescence should appear in the higher energy region than the ^1L_a fluorescence. It means that the fluorescence anisotropy should become larger (or closer to 0.4) at shorter wavelength. However, the observed wavelength dependence of the anisotropy is opposite. The fluorescence anisotropy becomes smaller (or closer to −0.2) at shorter wavelength.

The long-axis polarized component in the ^1L_a fluorescence is attributable to the ^1B_b-type fluorescence component that appears as a result of the vibronic coupling between the ^1L_a state and the ^1B_b state. In the Born−Oppenheimer approximation, the wave function of the ^1L_a state can be expressed as the product of the electronic and vibrational wave functions. With expanding the electronic wave function by Herzberg−Teller expansion, we obtain the following expression of the wave function of a vibrational level in the ^1L_a state:

$$|\Psi_L\rangle = |L_a(Q)\rangle|\nu(Q)\rangle_L = \left(|L_a(0)\rangle + \sum_e \sum_i \frac{\left\langle e(0)\left|\frac{\partial H}{\partial Q_i}\right|L_a(0)\right\rangle Q_i}{\Delta E} |e(0)\rangle + ... \right) |\nu_L(Q)\rangle \tag{3}$$

Here Q is the vibrational coordinate. In the second term, the contribution from the ^1B_b state is dominant when we discuss the optical transition between the ^1L_a state and the ground state. Therefore, eq 3 can be simplified as follows:

$$|\Psi_L\rangle \approx \left(|L_a(0)\rangle + \sum_i \frac{\left\langle B_b(0)\left|\frac{\partial H}{\partial Q_i}\right|L_a(0)\right\rangle Q_i}{\Delta E} |B_b(0)\rangle \right) |\nu_L(Q)\rangle \tag{4}$$

This is an expression showing that the fluorescence from the ^1L_a state can contain the B_b-type long-axis polarized component through the vibronic coupling. In polyacene, the oscillator strength of the ^1L_a state is much smaller than that of the ^1B_b state, so that the vibronic coupling should be taken into account when we discuss the $^1L_a \leftarrow S_0$ transition. Concerning anthracene, for example, Michl et al. carried out the polarization measurements of absorption in a stretched polymer film,[37] and Albrecht and co-workers reported polarization measurements of absorption and steady-state fluorescence in a 77 K glass matrix.[38] Both of these studies clearly showed that the ^1L_a band exhibits mixed polarization reflecting the vibronic coupling between the ^1L_a

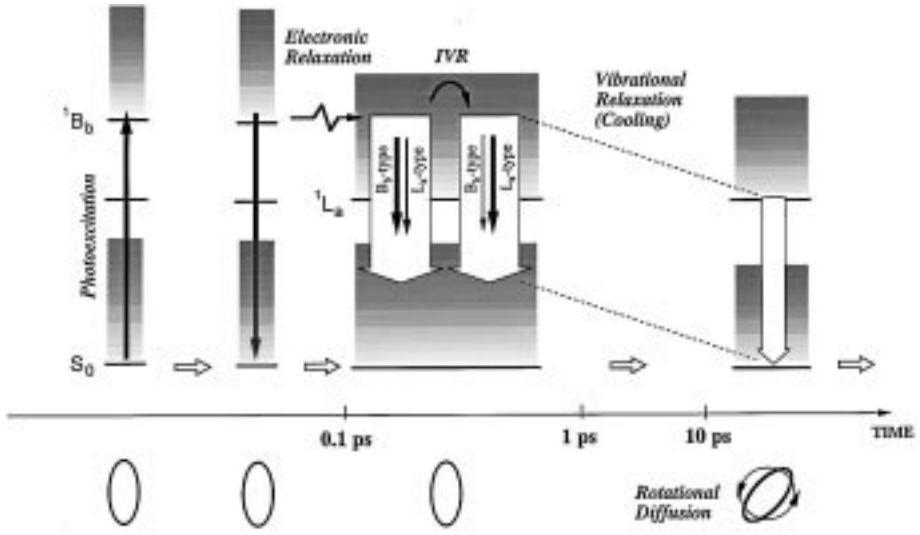

Figure 6. Schematic diagram depicting the relaxation processes of tetracene in solution following the direct photoexcitation to the highly excited singlet (S_n) state.

state and the ^1B_b state. In addition, it has been shown that the long-axis polarized component in the ^1L_a band becomes larger in the shorter wavelength in the absorption whereas it becomes bigger in the longer wavelength in the fluorescence. In polyacene (D_{2h}), the ^1L_a state and the ^1B_b state have B_{2u} and B_{3u} symmetry, respectively, so that these two states are vibronically coupled through b_{1g} vibrational modes. The spectrum of the ^1B_b-type component is shifted by one quantum of the b_{1g} vibration that is responsible for the vibronic coupling, because its spectrum is determined by the $\langle \nu_G|Q|\nu_L\rangle$ factor (G denotes the ground state) whereas the spectrum of the ^1L_a-type component reflects the Franck−Condon factor $\langle \nu_G|\nu_L\rangle$. Therefore, the ratio of the ^1B_b-type component changes with respect to the ^1L_a-type component when the wavelength changes. So far, the vibronic coupling has been discussed for the steady-state measurements of absorption and fluorescence, where the optical transition starts from thermally equilibrated molecules. In the femtosecond time region, on the other hand, we observe fluorescence from the highly excited vibrational state in the ^1L_a state of tetracene since the energy dissipation from the photoexcited molecule to the surrounding solvent does not occur significantly in this short time range. Nevertheless, it is highly likely that the arguments about the vibronic coupling are also applicable to the "hot fluorescence" that we observed. It should be noted that the visible fluorescence anisotropy observed for tetracene in the femtosecond region exhibits similar wavelength dependence to that observed for the vibronic ^1B_b-type component in the ^1L_a fluorescence of anthracene in a low-temperature glass matrix.[38] Thus, it can be safely concluded that the long-axis polarized component found in the visible fluorescence is due to the vibronic ^1B_b-type component in the fluorescence from the ^1L_a state.

The most important finding in the present study is the very rapid change of the visible fluorescence anisotropy in early delay time. This observation implies that the ratio of the vibronic ^1B_b-type component in the ^1L_a fluorescence is significantly larger initially after the electronic relaxation. In other words, the anisotropy data suggest that the highly excited vibrational states in the ^1L_a state which are strongly mixed with the ^1B_b state through the vibronic coupling are first populated preferentially when the molecule is relaxed from the ^1B_b state to the ^1L_a state and that the relaxation (or redistribution) to the other vibrational states takes place afterward in the ^1L_a electronic state.

3-6. Relaxation Processes of Photoexcited Tetracene. Figure 6 depicts a schematic diagram of the relaxation processes observed through the fluorescence intensity/anisotropy measurements of tetracene in the present study.

With absorbing a 273-nm photon, the molecule is first excited to the ^1B_b state, and the ^1B_b state emits fluorescence in the ultraviolet region. The ultraviolet ^1B_b fluorescence vanishes with a time constant of about 120 fs in accordance with the electronic relaxation to the ^1L_a state. Since the energy dissipation to the surrounding solvent can be neglected in this time scale, the $^1B_b \rightarrow {}^1L_a$ electronic relaxation can be considered to take place almost isoenergetically from the initially populated ^1B_b state(s) to the highly excited vibrational states of the ^1L_a state whose density of states is much higher. The fluorescence anisotropy data suggest that the electronic relaxation does not occur to all of the ^1L_a vibrational states equally even if they match the initially populated ^1B_b state in energy. The ^1B_b state(s) is preferentially relaxed to the vibrational states of the ^1L_a state which are strongly mixed with the ^1B_b state. The intramolecular vibrational redistribution process then takes place in the ^1L_a state, which gives rise to the rapid anisotropy change of the visible ^1L_a fluorescence in the femtosecond time region.

With the $^1B_b \rightarrow {}^1L_a$ electronic relaxation, the molecule gains large excess energy in the ^1L_a state, so that the ^1L_a fluorescence is initially emitted from the highly excited vibrational states. This "hot" fluorescence appears in almost the same energy region as the thermally equilibrated (or steady-state) ^1L_a fluorescence because the highly excited vibrational states in the ^1L_a state have significant Franck−Condon overlap (or the $\langle \nu_G|Q|\nu_L\rangle$ overlap for the ^1B_b-type component) only with highly excited vibrational states in the ground state. Nevertheless, reflecting some difference in the distribution of the Franck−Condon factor, the spectral shape of the hot fluorescence is slightly different from that of the thermally equilibrated (or steady-state) fluorescence. Consequently, the ^1L_a fluorescence spectrum changes with time in accordance that the molecule in the ^1L_a state is cooled by dissipating its excess energy to the surrounding solvent. This vibrational cooling process causes the ~12 ps dynamics that is observed as the wavelength-dependent temporal change of the fluorescence intensity. It may be worth mentioning that the "hot fluorescence" is not necessarily blue-shifted compared with thermally equilibrated fluorescence. The spectral change to be observed strongly depends on the potential

curves of the excited state and the ground state. In fact, the fluorescence intensity change observed for tetracene shows a tendency that the spectrum exhibits blue shift in accordance with the vibrational cooling. This blue shift can be easily rationalized if we assume that the potential curve of the ground state is steeper than that of the excited state. In addition, it is likely that the sharpening of the fluorescence band also contributes to the observed intensity change, which gives additional rising and decaying tendencies at the maxima and minima of the structured steady-state fluorescence. The rotational diffusion, on the other hand, takes place so that the fluorescence anisotropy vanishes with a time constant of a few tens of picoseconds.

An important question about the vibrational cooling process is whether it takes place after the excess energy is distributed over all vibrational modes statistically or not. In other words, the question is when the Boltzmann distribution over all of the vibrational states is achieved. Unfortunately, the present time-resolved fluorescence study cannot afford clear information about this problem. Time-resolved vibrational spectroscopic studies, such as picosecond anti-Stokes Raman measurements, are needed to investigate this problem.[35,39−41]

Finally, we mention the initial value of the visible fluorescence anisotropy. The observed value ranges from ~ 0 to ~ 0.07 for wavelengths of 546, 507, 474 nm. However, since the time constant of the rapid change of the anisotropy is comparable (or shorter) with our instrumental response, the deconvolution procedure is needed to obtain a real value. The present quality of data did not allow to carry out a reliable deconvolution procedure, but it is expected that the real value is even larger. The measurements having higher time resolution are required to determine the true initial value of the visible fluorescence anisotropy.

In conclusion, we measured femtosecond time-resolved fluorescence of tetracene with photoexcitation to the highly excited ^1B_b state and observed fluorescence from the ^1B_b state and the lowest excited ^1L_a state. Various types of fluorescence intensity/anisotropy dynamics were observed from the femtosecond to the picosecond time region, which reflect a series of the relaxation processes occurring in the molecule after photoexcitation. The present work clearly shows that femtosecond time-resolved fluorescence is highly capable not only of studying the S_1 state dynamics but also of examining the highly excited singlet states and their relaxation dynamics in solution.

Acknowledgment. The authors thank Prof. H. Baba for instructive and stimulating discussions. N.S. acknowledges the Japan Society for the Promotion of Science (JSPS) for a fellowship that allowed him to stay at IMS.

References and Notes

(1) Kasha, M. *Discuss. Faraday Soc.* **1950**, *9*, 14.
(2) Beer, M.; Longuet-Higgins, H. C. *J. Chem. Phys.* **1955**, *23*, 1390.
(3) Murata, S.; Iwanaga, C.; Toda, T.; Kokubun, H. *Chem. Phys. Lett.* **1972**, *13*, 101.
(4) Hirayama, F.; T. A. Gregory; Lipsky, S. *J. Chem. Phys.* **1973**, *58*, 4696.
(5) Katoh, R.; Fujiyoshi, S.; Kotani, M. *Chem. Phys. Lett.* **1998**, *292*, 621.
(6) Bogdanov, V. L. Fluorescence and Multiwave Mixing Induced by Photon Absorption of Excited State. In *Topics in Fluorescence Spectroscopy*; Lakowicz, J., Ed.; Plenum Press: New York, 1997; Vol. 5, p 211.
(7) Takeuchi, S.; Tahara, T. *J. Phys. Chem. A* **1997**, *101*, 3052.
(8) Tahara, T.; Hamaguchi, H. *Chem. Phys. Lett.* **1995**, *239*, 275.
(9) Takeuchi, S.; Tahara, T. *Chem. Phys. Lett.* **1997**, *277*, 340.
(10) Takeuchi, S.; Tahara, T. *J. Phys. Chem. A* **1998**, *102*, 7740.
(11) Kandori, H.; Sasabe, H.; Mimuro, M. *J. Am. Chem. Soc.* **1994**, *116*, 2671.
(12) Mimuro, M.; Akimoto, S.; Takaichi, S.; Yamazaki, I. *J. Am. Chem. Soc.* **1997**, *119*, 1452.
(13) Macpherson, A. N.; Gillbro, T. *J. Phys. Chem. A* **1998**, *102*, 5049.
(14) Azuma, J. *Chem. Phys. Lett.* **1998**, *288*, 77.
(15) Gurzadyan, G. G.; Tran-Thi, T.-H.; Gustavsson, T. *J. Chem. Phys.* **1998**, *108*, 385.
(16) Yoshizawa, M.; Suzuki, K.; Kubo, A.; Saikan, S. *Chem. Phys. Lett.* **1998**, *290*, 43.
(17) Platt, J. R. *J. Chem. Phys.* **1949**, *17*, 484.
(18) Klevens, H. B.; Platt, J. R. *J. Chem. Phys.* **1949**, *17*, 470.
(19) Tanaka, J. *Bull. Chem. Acta Jpn.* **1965**, *38*, 86.
(20) Grimme, S. *Chem. Phys. Lett.* **1996**, *259*, 128.
(21) Fleming, G. R.; Lewis, C.; Porter, G. *Chem. Phys. Lett.* **1975**, *31*, 33.
(22) Okajima, S.; Lim, E. C. *Chem. Phys. Lett.* **1976**, *37*, 403.
(23) Peter, G.; Bäsler, H. *Chem. Phys.* **1980**, *49*, 9.
(24) Wappelt, A.; Bergmann, A.; Napiwotzki, A.; Eichler, H. J.; Jüpner, H. J.; Kummrow, A.; Law, A.; Woggon, S. *J. Appl. Phys.* **1995**, *78*, 5192.
(25) Smith, A. W.; Weiss, C. *Chem. Phys. Lett.* **1972**, *14*, 507.
(26) Lopez-Delgado, R.; Miehe, J. A.; Sipp, B. *Opt. Commun.* **1976**, *19*, 79.
(27) Alfano, R. R.; Shapiro, S. L.; Pope, M. *Opt. Commun.* **1973**, *9*, 388.
(28) Fleming, G. R. *Chemical Applications of Ultrafast Spectroscopy*; Oxford University Press: New York, 1986.
(29) Ruggiero, A. J.; Todd, D. C.; Fleming, G. R. *J. Am. Chem. Soc.* **1990**, *112*, 1003.
(30) Wirth, M. J.; Chou, S.-H. *J. Phys. Chem.* **1991**, *95*, 1786.
(31) Brocklehurst, B.; Young, R. N. *J. Chem. Soc., Faraday Trans.* **1994**, *90*, 271.
(32) Kearvell, A.; Wilkinson, F. *Chem. Phys. Lett.* **1971**, *11*, 472.
(33) Horng, M. L.; Gardecki, J. A.; Papazyan, A.; Maroncelli, M. *J. Phys. Chem.* **1995**, *99*, 17311.
(34) Iwata, K.; Hamaguchi, H. *J. Phys. Chem. A* **1997**, *101*, 632.
(35) Elsaesser, T.; Kaiser, W. *Annu. Rev. Phys. Chem.* **1991**, *42*, 83.
(36) The total fluorescence intensities measured at parallel ($I_{||}$) and perpendicular ($I_\perp$) conditions are the sum of the two components that originate from the long- and the short-axis polarized transition moments, $I_{||} = I_{||}^{long} + I_{||}^{short}$ and $I_\perp = I_\perp^{long} + I_\perp^{short}$. A calculation for the ensemble of randomly oriented molecules shows that the above four quantities are related to I^{long} and I^{short} as follows:

$$I_{||}^{long} = \frac{1}{5} I^{long},\ I_\perp^{long} = \frac{1}{15} I^{long},\ I_{||}^{short} = \frac{1}{15} I^{short},\ \text{and}\ I_\perp^{short} = \frac{2}{15} I^{short}$$

We can directly obtain the eq 2 from these equations. Please note that we obtain

$$I_{||} + 2I_\perp = \frac{1}{3}(I^{long} + I^{short})$$

The factor of 1/3 reflects the fact that we can excite 1/3 of molecules by linearly polarized light.
(37) Michl, J.; Thulstrup, E. W.; Eggers, J. H. *Ber. Bunsen-Ges. Phys. Chem.* **1974**, *78*, 575.
(38) Friedrich, D. M.; Mathies, R.; Albrecht, A. C. *J. Mol. Spectrosc.* **1974**, *51*, 166.
(39) Matousek, P.; Parker, A. W.; Toner, W. T.; Towrie, M.; Faria, D. L. A. d.; Hester, R. E.; Moore, J. N. *Chem. Phys. Lett.* **1995**, *237*, 373.
(40) Graener, H.; Zürl, R.; Hofmann, M. *J. Phys. Chem. B* **1997**, *101*, 1745.
(41) Mizutani, Y.; Kitagawa, T. *Science* **1997**, *278*, 443.